

Computational Study of Excited-State Intramolecular-Proton-Transfer of *o*-Hydroxybenzaldehyde and Its Derivatives

Shin-ichi Nagaoka,*[1] Hiroyuki Teramae,[2] and Umpei Nagashima[3,4]

[1]Department of Chemistry, Faculty of Science and Graduate School of Science and Engineering, Ehime University, Matsuyama 790-8577

[2]Department of Chemistry, Faculty of Science, Josai University, 1-1 Keyakidai, Sakado 350-0295

[3]Research Institute for Computational Sciences, National Institute of Advanced Industrial Science and Technology, 1-1-1 Umezono, Tsukuba 305-8568

[4]CREST, Japan Science and Technology Agency, 4-1-8 Honcho, Kawaguchi 332-0012

Received November 10, 2008; E-mail: nagaoka@ehimegw.dpc.ehime-u.ac.jp

The excited-state intramolecular-proton-transfer of *o*-hydroxybenzaldehyde and its derivatives (*o*-formyl-substituted phenols) was studied by means of an ab initio molecular-orbital method. The computational results are consistent with the experimental fluorescence quantum yield and support the nodal-plane model. The energy difference between the ground state and the lowest excited $^1(\pi,\pi^*)$ state decreases as the electron-withdrawing property of a substituent bonded to the carbonyl carbon of *o*-hydroxybenzaldehyde becomes stronger. However, the substituent effect does not largely distort the potential energy surface of *o*-formyl-substituted phenols.

In a previous paper,[1] Nagaoka et al. discussed the excited-state intramolecular-proton-transfer (ESIPT)[2–5] of *o*-hydroxybenzaldehyde (OHBA) and related molecules in solution studied by emission spectroscopy. OHBA is the simplest aromatic molecule with intramolecular hydrogen-bonding involving a carbonyl group and can exist in two tautomeric forms: the keto form (normal form) and the enol form (proton-transferred form). In the ground state (S_0 state) the keto form is stable, but in the lowest excited $^1(\pi,\pi^*)$ state ($S_1^{(\pi)}$ state) ESIPT takes place and yields the enol form (Figure 1). The observed behavior concerning ESIPT of OHBA and related molecules can be explained by considering the nodal pattern of the wave function along with the delocalization of the π electrons in the excited state (nodal-plane model,[1,6–8] see the Supporting Information). Although our nodal-plane model is qualitative, it allows us to immediately recognize the important feature of ESIPT of various molecules and provides useful information about the reaction mechanisms of ESIPT.

Our nodal-plane model was previously applied to the substituent effect on the $S_1^{(\pi)} \rightarrow S_0$ fluorescence quantum yields of *o*-formyl-substituted phenols (OHBAs).[1] The fluorescence quantum yield decreases as the electron-withdrawing property of a substituent bonded to the carbonyl carbon of OHBA becomes stronger. From this experimental result together with the energy gap law, it was suggested that the energy difference between the zero-point vibrational levels of the $S_1^{(\pi)}$ and S_0 states decreases as the electron-withdrawing property becomes stronger.[1] On the other hand, our nodal-plane model shows that the substituent effect does not largely distort the potential energy surface of OHBAs but only reduces the $S_0 \rightarrow S_1^{(\pi)}$ and $S_1^{(\pi)} \rightarrow S_0$ transition energies as the electron-withdrawing property becomes stronger (Figure 4S of the Supporting Information).[1] Thus, our nodal-plane model is consistent with the suggestion derived from the experimental results of the fluorescence quantum yield. However, the

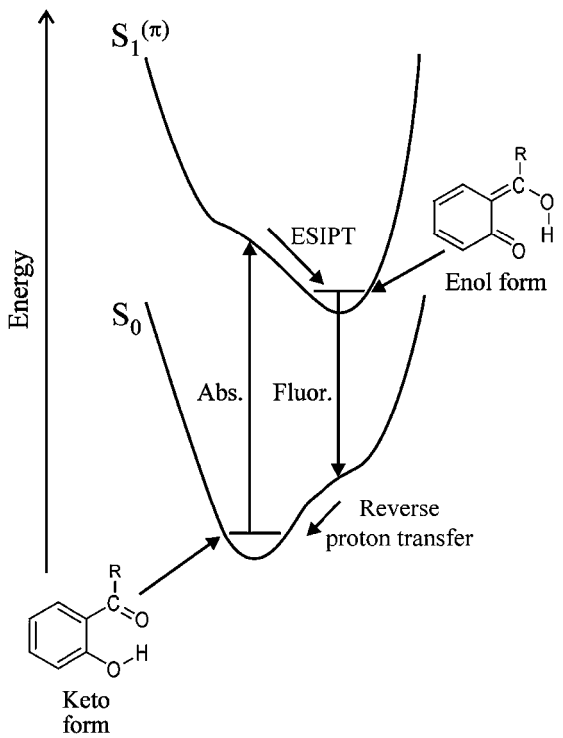

Figure 1. Schematic representation of potential energy curves for the S_0 and $S_1^{(\pi)}$ states of OHBAs. "Abs." and "Fluor." denote absorption and fluorescence-emission, respectively.

Published on the web May 13, 2009; doi:10.1246/bcsj.82.570

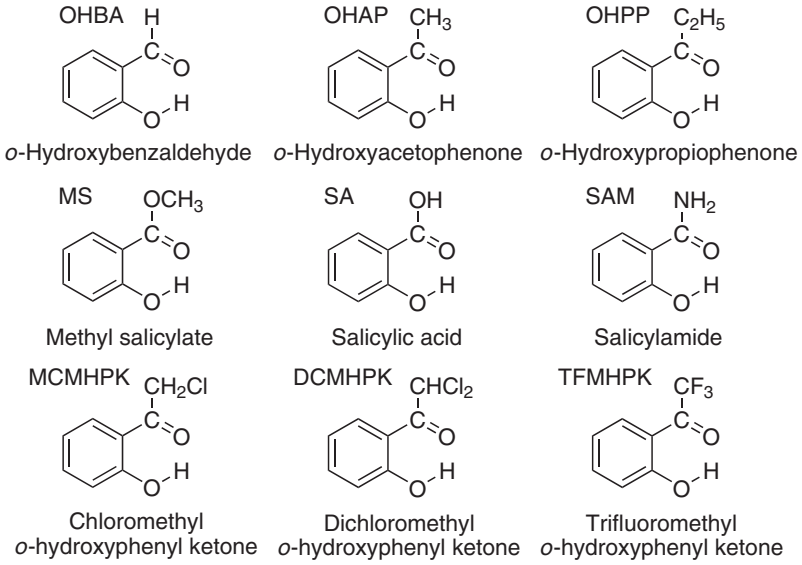

Figure 2. Structures of OHBAs studied in the present work.

previous experimental results of OHBAs are limited to the substituent effect on the fluorescence quantum yield, and there is no direct and reliable experimental indication of the substituent effect on the potential energy surface because the electronic spectra (especially the fluorescence spectra) are broad owing to ESIPT.[1,6,7]

Accordingly, in this work, we have performed ab initio calculations of OHBAs to discuss the substituent effect on the potential energy surface. Although we previously carried out ab initio calculations for the S_0 and $S_1^{(\pi)}$ states of OHBA,[7] the basis set used there was poor (STO-3G). Although computational dynamics of a few OHBAs was recently studied,[9] the above-mentioned substituent effect has not been elucidated sufficiently. So we have here investigated the substituent effect by using some post Hartree–Fock methods and reasonable-size basis sets. The structures of the molecules studied in this work are shown in Figure 2.

Computational Method and Procedure

The ab initio molecular-orbital calculations of OHBA, *o*-hydroxyacetophenone (OHAP), *o*-hydroxypropiophenone (OHPP), methyl salicylate (MS), salicylic acid (SA), salicylamide (SAM), chloromethyl *o*-hydroxyphenyl ketone (MCMHPK), dichloromethyl *o*-hydroxyphenyl ketone (DCMHPK), and trifluoromethyl *o*-hydroxyphenyl ketone (TFMHPK) were mainly done at the CIS/6-31G**//HF/6-31G** and CIS/6-31G**//CIS/6-31G** levels for the S_0 and $S_1^{(\pi)}$ states, respectively, using the Gaussian 03 program.[10] We tried to optimize the structures for both of the keto and enol forms for each of the S_0 and $S_1^{(\pi)}$ states. Since all of the vibrational frequencies for the optimized structures thus obtained were positive, we thought that the optimizations did not give structures for saddle points but gave those for local minima. All of the optimized structures were planar.

We confirmed our basis set quality by comparing the above results of OHBA with those obtained by using the 6-311G** basis set. The activation energies of the keto → enol and enol → keto isomerizations in the S_0 state were respectively

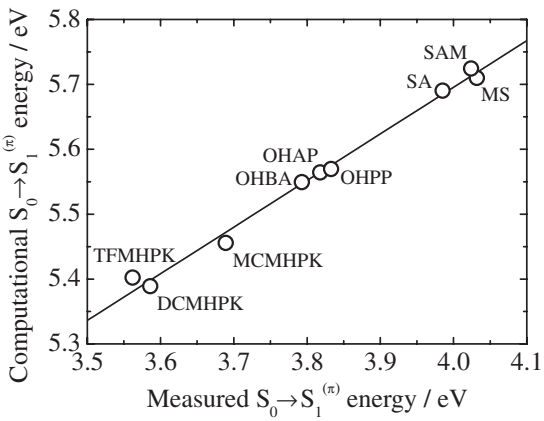

Figure 3. Relation between measured $S_0 \rightarrow S_1^{(\pi)}$ transition energies of OHBAs[1] and their computational values at the CIS/6-31G**//HF/6-31G** level. The plot gives a good linear fit with a slope of 0.718, an intercept of 2.82, and a correlation coefficient of 0.996.

obtained to be 18.7 and 2.3 kcal mol^{-1} (1 kcal mol^{-1} = 4.184 kJ mol^{-1}) at the HF/6-31G** level, and they were 19.0 and 2.8 kcal mol^{-1} at the HF/6-311G** level. For our purpose, no significant difference was observed between the 6-31G** and 6-311G** results. Furthermore, to check the electron correlation effect on the enol form in the S_0 state of OHBAs, we performed the geometry optimization of OHBA at the MP2/6-311G** and B3LYP/6-31G** levels as noted in the next section. The correlation effects on the keto and enol structures for the S_0 and $S_1^{(\pi)}$ states of OHBA were also checked at the CASSCF(8,8)/6-31G** level (see the Supporting Information), where the number of the configuration state function was 1764 and all of the vibrational frequencies for the optimized structures were positive.

The $S_0 \rightarrow S_1^{(\pi)}$ and $S_1^{(\pi)} \rightarrow S_0$ transition energies of OHBAs were calculated for the optimized structures of the keto and enol forms for the S_0 and $S_1^{(\pi)}$ states, respectively.

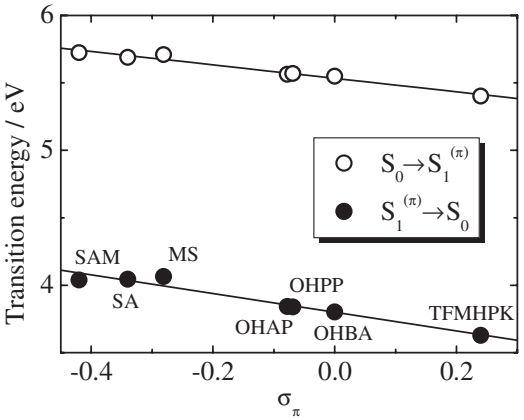

Figure 4. Plots of computational $S_0 \rightarrow S_1^{(\pi)}$ and $S_1^{(\pi)} \rightarrow S_0$ transition energies of OHBAs at the CIS/6-31G**//HF/6-31G** and CIS/6-31G**//CIS/6-31G** levels as a function of σ_π for the substituent bonded to the carbonyl carbon of OHBA. The plots for the $S_0 \rightarrow S_1^{(\pi)}$ and $S_1^{(\pi)} \rightarrow S_0$ transitions give good linear fits with slopes of -0.499 and -0.693, intercepts of 5.53 and 3.80, and correlation coefficients of 0.985 and 0.975, respectively.

Figure 3 shows a relation between the measured[1] and computational $S_0 \rightarrow S_1^{(\pi)}$ transition energies. Although the quantitative agreement between the measured and computational values is not satisfactory, this plot indicates a linear relationship, suggesting that our estimation of the transition energies has been made appropriately.

Results and Discussion

In Figure 4, the computational $S_0 \rightarrow S_1^{(\pi)}$ and $S_1^{(\pi)} \rightarrow S_0$ transition energies of OHBAs are plotted as a function of Yukawa and Tsuno's σ_π constant[11–13] for the substituent bonded to the carbonyl carbon. σ_π is a type of Hammett parameter and the resonance substituent constant, measuring the capability for π-delocalization of a π-electron-donating or π-electron-withdrawing substituent. As the electron-withdrawing property of a substituent bonded to the carbonyl carbon becomes stronger, σ_π increases. Since the change in electronic structure due to the $S_0 \rightarrow S_1^{(\pi)}$ excitation [(π,π^*) transition] primarily affects the π-bonding framework,[1,6–8] the σ_π constant is the most suitable choice as the Hammett parameter for analyzing the present computational results.

Each plot in Figure 4 shows a good linear relationship with a negative slope, so that as σ_π increases, the transition energy decreases. These computational results are consistent with the suggestion derived from the experimental fluorescence quantum yields of OHBAs, and support our interpretation based on the nodal-plane model given in a previous paper:[1] our nodal-plane model predicted that the transition energy decreases as the electron-withdrawing property of the substituent bonded to the carbonyl carbon becomes stronger. The change in π gross orbital charge due to the substitution is not localized at the carbonyl carbon but delocalized over the whole molecule.

If these substituent effects based on our nodal-plane model were absent, the transition energies would not show systematic dependence on the electron-donating and electron-withdrawing

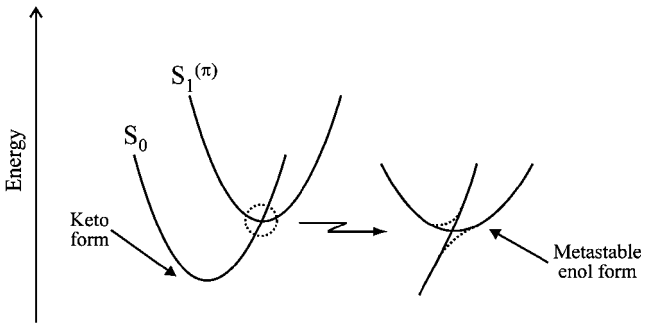

Figure 5. Schematic drawing of a zero-order potential-surface crossing between the S_0 and $S_1^{(\pi)}$ states in OHBA, MCMHPK, DCMHPK, and TFMHPK. The crossing is drawn in an exaggerated way.

properties of the substituent. In fact, the $S_0 \rightarrow S_1^{(\pi)}$ transition energies of benzene, trifluoromethylbenzene (Ph–CF_3), toluene (Ph–CH_3), and anisol (Ph–OCH_3) were calculated to be 6.36, 6.32, 6.29, and 6.22 eV, respectively. These values do not show a systematic substituent effect, in contrast to those of OHBAs shown in Figure 4.

The plots for the $S_0 \rightarrow S_1^{(\pi)}$ and $S_1^{(\pi)} \rightarrow S_0$ transition energies are nearly parallel to each other in Figure 4. Thus, the substituent effect does not largely distort the potential energy surface of OHBAs but changes only the energy difference between the zero-point vibrational levels of the $S_1^{(\pi)}$ and S_0 states: the difference in length between the two arrows (Abs. and Fluor.) in Figure 1 is nearly constant among OHBAs. These computational results are also consistent with our nodal-plane model.

Although the potential energy surface for the S_0 state of OHBA was thought to have a single minimum in a previous paper,[7] the optimized structure of the enol form in the S_0 state has been obtained for OHBA, MCMHPK, DCMHPK, and TFMHPK in this work (see the Supporting Information). This can be explained in terms of a zero-order potential-surface crossing between the S_0 and $S_1^{(\pi)}$ states (Figure 5). It is thought that the zero-order potential-surface of the $S_1^{(\pi)}$ state is lowered in OHBA, MCMHPK, DCMHPK, and TFMHPK, and crosses that of the S_0 state. To help the reader's understanding, in Figure 5 the crossing is drawn in an exaggerated way. The crossing reduces $S_1^{(\pi)} \rightarrow S_0$ fluorescence quantum yield in these molecules. Such a crossing is, however, absent in the other molecules. The lowering of the zero-order potential-surface of the $S_1^{(\pi)}$ state of a molecule with large σ_π (π-electron-withdrawing substitution) can be explained by considering our nodal-plane model as described previously.[1] The activation energies of the keto $\rightarrow$ enol isomerizations in the S_0 state were found to be 18.7, 18.1, 19.2, and 19.9 kcal mol^{-1} for OHBA, MCMHPK, DCMHPK, and TFMHPK, respectively, at the HF/6-31G** level. Since those of the enol $\rightarrow$ keto transformations were small (2.3, 1.3, 0.8, and 1.3 kcal mol^{-1}, respectively), the crossing and distortion of the potential energy surfaces did not clearly manifest themselves in the plot for the $S_1^{(\pi)} \rightarrow S_0$ transition energy in Figure 4. Zero-point-energy correction eliminated the potential barrier of the enol $\rightarrow$ keto isomerization in the S_0 state. Furthermore, inclusion of electron correlation effects at the MP2/6-311G** or B3LYP/6-31G**

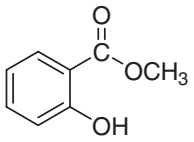

Chart 1.

level also eliminated the enol-type local minimum of OHBA, and only the keto form was optimized. The optimized keto-forms at these levels of OHBA were similar to that at the HF/6-31G** level (see the Supporting Information). These more reliable calculations support the qualitative nature of the potential energy surface shown in Figure 1.

Weller proposed that a dynamic equilibrium between the normal (keto) and proton-transferred forms occurs in the $S_1^{(\pi)}$ state of MS and the two forms fluoresce in UV and visible regions.[14] However, Sandros showed that the equilibrium is almost totally displaced to the proton-transferred form in the $S_1^{(\pi)}$ state and the origin of the UV fluorescence is not the keto form but the $COOCH_3$ rotamer (Chart 1).[15] Contrary to general expectations (for example, see Ref. 3), in this work the optimized structure of the keto form in the $S_1^{(\pi)}$ state was obtained for MS and SA (see the Supporting Information). The keto forms in the $S_1^{(\pi)}$ states of MS and SA were a little more stable than the enol forms (by 0.5 and 0.8 kcal mol^{-1}, respectively), and the activation energies of the keto $\rightarrow$ enol isomerizations were obtained to be 5.1 and 5.4 kcal mol^{-1} in MS and SA, respectively. It is interesting whether such a keto form shows fluorescence emission or not. The rotamers (Chart 1) for the S_0 and $S_1^{(\pi)}$ states of MS (see the Supporting Information) were respectively by 3.4 and 6.1 kcal mol^{-1} more unstable than the keto forms, and the fluorescence emission of the rotamer (5.26 eV) was expected to be blue-shifted from that of the enol form (4.06 eV). The blue-shift is qualitatively consistent with the experimental result.[15]

Conclusion

ESIPT of OHBAs was studied by means of an ab initio molecular-orbital method. The computational results are consistent with the experimental fluorescence quantum yield and support our nodal-plane model. The substituent effect does not largely distort the potential energy surface of OHBAs but only reduces the energy difference between the zero-point vibrational levels of the $S_1^{(\pi)}$ and S_0 states as the electron-withdrawing property of a substituent bonded to the carbonyl carbon of OHBA becomes stronger.

We thank Mr. Daishiro Hashizume and Ms. Wakana Fujita of Josai University for their help in the early stage of this work. S.N. thanks the Research Center for Computational Science at the Okazaki Research Facilities of the National Institutes of Natural Sciences for the use of the computers and the Library Program Gaussian 03. This work was partly supported by a Grant-in-Aid for Scientific Research (C) (No. 19550020) from the Japan Society for the Promotion of Science (JSPS).

Supporting Information

Description of the nodal-plane model, the optimized structures of the keto and enol forms for the S_0 and $S_1^{(\pi)}$ states of OHBA at the CASSCF(8,8)/6-31G** level together with those at the HF/6-31G** and CIS/6-31G** levels, the optimized keto-forms at the MP2/6-311G** and B3LYP/6-31G** levels for the S_0 state of OHBA, the optimized enol-form for the S_0 state of OHBA at the HF/6-31G** level, the optimized keto-forms for the $S_1^{(\pi)}$ states of MS and SA at the CIS/6-31G** level, and the optimized rotamers for the S_0 and $S_1^{(\pi)}$ states of MS at the HF/6-31G** and CIS/6-31G** levels are included in Supporting Information. This material is available free of charge on the web at http://www.csj.jp/journals/bcsj/.

References

1 S. Nagaoka, A. Nakamura, U. Nagashima, *J. Photochem. Photobiol., A* **2002**, *154*, 23.

2 P. F. Barbara, P. K. Walsh, L. E. Brus, *J. Phys. Chem.* **1989**, *93*, 29.

3 S. J. Formosinho, L. G. Arnaut, *J. Photochem. Photobiol., A* **1993**, *75*, 21.

4 T. Sugawara, I. Takasu, *Adv. Phys. Org. Chem.* **1999**, *32*, 219.

5 P.-T. Chou, *J. Chin. Chem. Soc.* **2001**, *48*, 651.

6 S. Nagaoka, U. Nagashima, N. Ohta, M. Fujita, T. Takemura, *J. Phys. Chem.* **1988**, *92*, 166.

7 S. Nagaoka, U. Nagashima, *Chem. Phys.* **1989**, *136*, 153.

8 S. Nagaoka, A. Fujii, M. Hino, M. Takemoto, M. Yasuda, M. Mishima, K. Ohara, A. Masumoto, H. Uno, U. Nagashima, *J. Phys. Chem. B* **2007**, *111*, 13116, and references cited therein.

9 J. D. Coe, T. J. Martinez, *Mol. Phys.* **2008**, *106*, 537, and references cited therein.

10 M. J. Frisch, G. W. Trucks, H. B. Schlegel, G. E. Scuseria, M. A. Robb, J. R. Cheeseman, J. A. Montgomery, Jr., T. Vreven, K. N. Kudin, J. C. Burant, J. M. Millam, S. S. Iyengar, J. Tomasi, V. Barone, B. Mennucci, M. Cossi, G. Scalmani, N. Rega, G. A. Petersson, H. Nakatsuji, M. Hada, M. Ehara, K. Toyota, R. Fukuda, J. Hasegawa, M. Ishida, T. Nakajima, Y. Honda, O. Kitao, H. Nakai, M. Klene, X. Li, J. E. Knox, H. P. Hratchian, J. B. Cross, V. Bakken, C. Adamo, J. Jaramillo, R. Gomperts, R. E. Stratmann, O. Yazyev, A. J. Austin, R. Cammi, C. Pomelli, J. W. Ochterski, P. Y. Ayala, K. Morokuma, G. A. Voth, P. Salvador, J. J. Dannenberg, V. G. Zakrzewski, S. Dapprich, A. D. Daniels, M. C. Strain, O. Farkas, D. K. Malick, A. D. Rabuck, K. Raghavachari, J. B. Foresman, J. V. Ortiz, Q. Cui, A. G. Baboul, S. Clifford, J. Cioslowski, B. B. Stefanov, G. Liu, A. Liashenko, P. Piskorz, I. Komaromi, R. L. Martin, D. J. Fox, T. Keith, M. A. Al-Laham, C. Y. Peng, A. Nanayakkara, M. Challacombe, P. M. W. Gill, B. Johnson, W. Chen, M. W. Wong, C. Gonzalez, J. A. Pople, *Gaussian 03, Revision C.02*, Gaussian, Inc., Wallingford CT, **2004**.

11 N. Inamoto, *Hammett Rule*, Maruzen, Tokyo, **1983**.

12 C. D. Johnson, *The Hammett Equation*, Cambridge University, London, **1973**.

13 Y. Tsuno, M. Fujio, *Chem. Soc. Rev.* **1996**, *25*, 129.

14 A. Weller, *Z. Elektrochem.* **1956**, *60*, 1144.

15 K. Sandros, *Acta Chem. Scand., Ser. A* **1976**, *30*, 761.